Biogeochemistry **9**: 75–98, 1990

Pyrite accumulation in salt marshes in the Eastern Scheldt, southwest Netherlands

OENE OENEMA
Netherlands Fertilizer Institute, c/o Institute for Soil Fertility, P.O. Box 30003, 9750 RA Haren, The Netherlands

Key words: pyrite formation, pyrite oxidation, framboids, salt marsh, sulfide, reducible iron, Eastern Scheldt

Abstract. Pore water composition, pyrite distribution and pyrite crystal morphology of sediments from salt marshes in the Eastern Scheldt, southwestern Netherlands, were examined from July 1984 to October 1986.

Hydrology and marsh vegetation were the chief determinants of pyrite accumulation. In the bare sediments of pans in the low marsh, highly reducing conditions prevailed just below the surface. At these sites, practically all the incoming detrital pyrite (0.5–1% FeS_2) was preserved. The in-situ formation of pyrites was negligible in these anoxic sediments.

All incoming detrital pyrite was oxidized in the surface layers (0–10 cm) of the medium-high marsh overgrown with *Spartina anglica*. Pyrite was formed at a rate of 2.6–3.8 mol S-FeS_2 m^{-2} yr^{-1} in a narrow range of depths (15–20 cm), at the interface of the oxidizing and underlying reducing sediment. At this interface the concentration profiles of Fe^{2+} and dissolved ΣS intersected. The role of the rhizosphere is discussed in connection with pyrite formation. No further pyrite formation occurred deeper in the sediment. This resulted in the build up of high concentrations of dissolved ΣS and acid volatile sulfides (AVS). The decrease with depth in oxalate-extractable Fe indicated that most of the iron oxyhydroxides (70–80%) had been transformed to pyrite. Another 10–20% of oxalate-extractable Fe was present as AVS. The abundance of framboidal pyrite particles and the high concentrations of AVS and dissolved ΣS indicated that the formation of pyrite occurred via iron monosulfide intermediates.

There was a linear relationship between the organic carbon and the S-FeS_2 content in the *Spartina* overgrown reducing sediment. The mean C/S ratio was 4.2.

Introduction

In organically-rich marine sediments, large quantities of sulfides are produced by organic matter oxidation through bacterial sulfate reduction. Generally, the greater part of the sulfides are reoxidized again to sulfate at the oxic-anoxic interface of the sediment. A significant portion, however, reacts with iron oxyhydroxides to form pyrite (FeS_2) (Berner 1970, 1984; Rickard 1974). Under reducing conditions pyrite is stable and preserved over geological time, storing large quantities of energy (Howarth 1984) and

potential acidity (Van Breemen 1976; Van Breemen et al. 1983). Under oxidizing conditions pyrite decomposes rapidly. This process may have serious environmental consequences because of the associated acidification.

Saltmarshes are characterized by large inputs of organic matter, which support high rates of bacterial sulfide production (Howarth & Teal 1979; Howes et al. 1984). Moreover, tidal rhythm, root metabolism of the marsh vegetation and atmospheric exposure induce dynamic redox conditions in the surface layers of saltmarsh sediments (Lord 1980; Howes et al. 1981; Feijtel et al. 1988). Such environments provide appropriate conditions for the accumulation of sedimentary pyrite.

The process of pyrite formation in salt marshes is not well understood. Euhedral pyrite is formed directly (Rickard 1975; Luther et al. 1982), and framboidal pyrite indirectly via iron monosulfide intermediates (Sweeney & Kaplan 1973; Raiswell 1982). The direct reaction pathway proceeds rapidly and has been reported to occur in salt marshes (Howarth 1979), but framboidal pyrite formation has also been observed in salt marshes (Lord 1980) and mangrove swamps (Van Breemen 1976).

The present study concerns the accumulation of pyrite in salt marshes of the Eastern Scheldt, a tidal inlet in the delta of south-western Netherlands. Results of microscopic observation were combined with solid phase analyses of sulfide species, so as to infer the pathway of pyrite formation. Hydrological observations and chemical analyses of the pore waters sampled from July 1984 to October 1986 were used to study the dynamics of the Fe-S geochemistry of bare- and *Spartina anglica*-overgrown marsh sediments.

Methods

The study sites

Salt marshes (16 km^2) occur in sheltered places alongside the dikes surrounding the Eastern Scheldt (Fig. 1). The flooding frequency of the marshes varied with the height of the marsh surface (Table 1). The considerable reduction in tide range in 1985–1986, during the final phase of construction of the Storm Surge Barrier (Knoester et al. 1984), strongly reduced the flooding frequency of the marshes. *Spartina anglica* was the dominant vegetation type of the low and medium-high marsh. On the high marsh the relatively species-rich vegetation was dominated by *Triglochin maritima, Limnonium vulgare, Puccinellia maritima* and *Halimione portulacoides*. Pyrite accumulation in marsh sediments was studied at 4 sites in 1984–1986. The main study-site was the Rattekaai marsh (Fig. 1), because

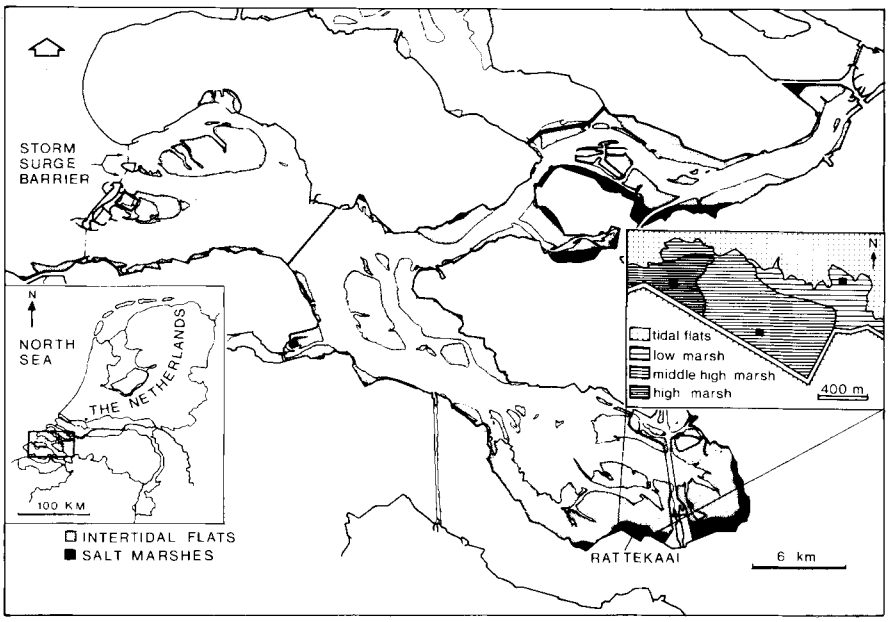

Fig. 1. Location of saltmarshes in the Eastern Scheldt. Inset shows study sites in the Rattekaai marsh.

conditions in this marsh are rather well documented (Kooistra 1978, 1981; Oenema & DeLaune 1988).

Sediment sampling and analysis

A total of 17 cores were analyzed to study the spatial and temporal variation in pyrite distribution with depth. Cores were taken by slowly twisting a thin walled PVC tube (i.d. 10–16 cm) into the marsh. The tube had a sharpened, serrated end to cut through plant roots. Within 4 hours after sampling the cores were sliced into 1–5 cm sections and these were dried at 80 °C for 72 hrs. All further sediment analyses were carried out on the dried and finely ground samples.

Organic carbon was determined by wet oxidation with $K_2Cr_2O_7$ and H_2SO_4 (Page et al. 1982). The oxidation of FeS_2 in pyritic (1–2%) sediments during the carbon oxidation may have caused an overestimation of the carbon content of 0.3–0.7%, but not more.

Pyrite was determined using the selective dissolution method described by Begheyn et al. (1978). A subsample of 100 mg was first treated with H_2SO_4 (96%) and HF (48%) for 1 min. and then with hot 4 M HCl for 10–30 min

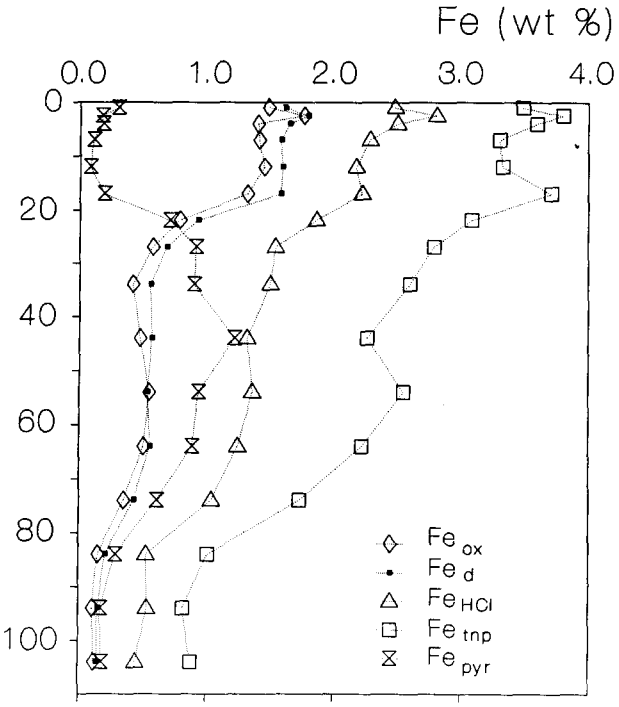

Fig. 2. Depth distribution of iron-species in core B10 from the medium-high marsh. Fe_{pyr} is pyrite-Fe, Fe_{ox} is oxalate-extractable Fe, Fe_d is dithionite-extractable Fe, Fe_{HCl} is hot HCl-extractable Fe, Fe_{tnp} is total non-pyritic Fe.

to dissolve all remaining non-pyritic iron. After centrifugation and washing 3 times with 1 M HCl the pyritic residue was dissolved in HNO_3. The total Fe and Fe-FeS_2 were determined by AAS. Analyses of split samples that were dried at 80 °C and freeze-dried gave similar pyrite concentrations, suggesting that drying at 80 °C did not oxidize FeS_2 to a noticeable extent in these samples. A molar S/Fe ratio of 2.007 ($n = 61$; $R^2 = 0.98$) in one series of samples, analyzed by standard ICP techniques, confirmed the pyrite-like composition of the residue. The recovery of a finely powdered FeS_2 crystal (purity > 99%), added to a sediment was 98 $\pm$ 1.5% ($n = 23$).

Several methods were compared for the determination of 'easily reducible iron'. Results for core B10 from the medium-high marsh are shown in Fig. 2. The extraction with 1 M Na-citrate + $Na_2S_2O_4$ (Holmgren 1967) yielded about half as much as the extraction with H_2SO_4, HF and HCl (Begheyn et al. 1978) suggesting that about 50% of the non-pyritic Fe was linked with the alumino-silicate minerals (i.e., illites and smectites). The other half of the

non-pyritic Fe consisted of iron oxyhydroxides and iron monosulfides. The latter oxidized during the drying procedure into easily extractable oxyhydroxides. The extraction with NH_4-oxalate (1 M, pH 3; Schwertmann, 1964) yielded only slightly less Fe (0–20%) than with the more aggressive citrate-extraction, suggesting that most oxyhydroxides were not well crystallized. In support of this opinion, X-ray diffraction analysis before and after oxalate-extraction (Schulze 1981) gave no indications of goethite or hematite. Extractions with hot concentrated HCl (Berner 1970) included also silicate-bound Fe since 0.3–1.0% more Fe was extracted than with oxalate and dithionite (Fig. 2). Iron oxyhydroxides and especially amorphous hydroxides (e.g., ferrihydrites) become preferentially sulfidized, since the weathering rate of Fe from silicates is much slower than it is from the X-ray amorphous oxyhydroxides in a sulfidic environment (e.g., Berner 1970; Lord & Church 1983). The degree of pyritization (DOP) as used in this study is therefore defined as:

$$\text{DOP} = \frac{\%\text{Fe-FeS}_2}{\%\text{Fe-FeS}_2 + \%\text{Fe}_{ox}} \quad (1)$$

where Fe_{ox} = the oxalate extractable Fe content

FeS_2 was shown not to dissolve by the oxalate extraction. Some of the data presented recently by Phillips and Lovley (1987) suggest that oxidation during the drying and analysis procedures of reduced sediments may diminish the total oxalate-extractable Fe. If so, the DOP calculated according to Eq. 1 is an overestimate.

Acid volatile sulfides (AVS) were determined in 2 ml of sediment. After the volatilization by the addition of 2 ml 5 M HCl the AVS were distilled over in two Zn-acetate traps using N_2 as a carrier gas. The distillation was continued for 1 hr. The quantity of sulfide so collected was analyzed by iodimetric titration (Bassett et al. 1978).

Major elements (Si, Al, Ca, Mg, K, Fe) were determined by XRF in 0.5 g sample of ignited (950 °C) sediment, mixed thoroughly with 5 g Spectroflux type 1100 (Johnson Matthey Chemicals, England) and then melted at 1200 °C to a disc.

Microscopic observations of pyrite and pyrite oxidation products were made on 15 × 8 cm^2 thin sections. The large thin sections were sampled from undisturbed sediment cores (i.d. 16 cm) and thereafter immediately freeze-dried, prior to impregnation and preparation (Kooistra 1978). For scanning electron microscopy (SEM) studies, impregnated sections (2 × 5 cm^2) were polished, coated with carbon and run on a Cambridge Steroscan S180 with a Link energy dispersive unit (EDS).

Pore water sampling and analysis

Seasonal variations in the pore water composition were measured at three sites in the Rattekaai marsh, one of them at the medium-high and two at the low level (one vegetated and one unvegetated). Pore water was sampled by in-situ dialysis, using a modification of the Hesslein in-situ sampler (Hesslein 1976) as described in detail by Oenema (1988b). In summary, the sampler was filled with 20–40 ml de-oxygenated, filtered seawater and left for 1–2 months to equilibrate with the surrounding pore water through a Versapor 200 (Gelman Sciences) filter-membrane (0.2 μm pore-diameter), then 2–10 ml portions were sucked into three syringes via sample ports at the surface. Tygon tubes (i.d. 0.8 mm) connected the sample ports with the 20 sample compartments at 0.5–5 cm intervals, in the sampler. One syringe contained 5 ml of 0.1 M H_2SO_4 and was used for Fe^{2+} analysis. Another syringe was prefilled with 2 ml of Zn-Acetate (2%) and 0.5 ml of 0.5 M NaOH and was used for dissolved sulfide (ΣS) analysis. After sampling, all compartments were immediately refilled with filtered, de-oxygenated seawater. The sampler remained permanently in the sediment, so as to avoid confounding seasonal changes with spatial variability. The concentrations of Cl^- (mercury thiocyanate; Zall et al., 1956), SO_4^{2-} (methylthymol blue; Merks & Sinke 1981) and Fe (2,4,6,-tripyridyl-(2)-1,3,5,-triazine-hydroxylamine; Henriksen 1967) were analyzed by standard auto-analyzer techniques. The concentration of ΣS was determined using the methylene-blue method of Gilboa-Garber (1971). The pH (NBS-scale) was determined in 2 ml of pore water with a micro-electrode within 3 hrs after sampling.

Hydrological observations

The depth of the water table was measured during low tide in bore-holes (i.d. 6 cm), two hours after they had been made. The pore water entered the hole rapidly, and changes in the water level after two hours were negligible.

Creek bank seepage was measured 3 times during the period October 1984 to February 1985 at 6 sites in the Rattekaai marsh. The seepage water was collected during low tide in 0.5 m long gutters that were placed carefully in the creek wall, just above the creek bottom. The volume of seepage water was measured after 2–3 hours.

Water retention characteristics of undisturbed backmarsh and levee samples in 100 cm^3 cores were determined over the range $\log|h| = 0$ to $\log|h| = 2$, where h = matrix suction (cm). After the initial water saturation for three weeks by inundation, the samples were placed on a fine-textured sand and equilibrated at $|h| = 2.5$, 10, 31, 63 and 100 cm, respectively (Klute 1986). After equilibrium had been reached, as indicated by a

constant sample weight (usually within 1 week), the water loss (in grams per 100 cm^3) was calculated from the difference in weight. These measurements were repeated 2 times in the range from $\log|h| = 0$ to $\log|h| = 2$ with the same samples. Between each cycle the samples were saturated by inundation for 3 weeks.

Results and discussion

Pyrite depth profiles

Figure 3A shows the FeS_2 distribution with depth at 4 backmarsh sites in the Rattekaai marsh. These distributions may be explained by the simultaneous occurrence of 3 processes:

1. sedimentation of pyrite-containing material,
2. pyrite oxidation in the upper rooting zone,
3. pyrite formation at the transition from the suboxic to the anoxic zones.

The current fine-grained sediments in the Eastern Scheldt originated mainly from erosion material of subrecent pyritic deposits exposed elsewhere in the Eastern Scheldt (Oenema 1989). Consequently, surface layers (0–1 cm) formed by this material contained 0.5–1% FeS_2. The microscopic detection (SEM-XDRA) of FeS_2 in suspended matter filtered from flood currents near the Rattekaai marsh (Kooistra 1981) is consistent with the proposed role of sedimentation processes in pyrite accumulation. This surface layer pyrite was preserved in the reducing and rapidly accreting fine-grained sediments of mussel banks and abandoned channels (Oenema 1988a), but oxidized in the upper rooting zone of the marsh sediments (Figs. 3, 4).

The oxidizing conditions in the upper rooting zone were probably caused by oxygen intrusion in the sediment via roots of plants such as *Spartina anglica*, as suggested by Gleason & Zieman (1981) and Mendelsohn et al. (1981) and via diffusion of air through pores, drained during low tide (Dacey & Howes 1984). Pyrite oxidation was not evident in the low marsh (Fig. 3A), but it was in the medium-high and high marsh and the natural levees (Fig. 4). The medium-high marsh was oxidizing (with positive Eh) in the upper 5–10 cm and reducing (with negative Eh) below 15 cm (Fig. 5). The surface sediments of the low marsh were less oxidizing. The differences in redox potentials between the low marsh and the medium-high marsh were related to the differences in flooding frequency (Table 1) and in growth of *Spartina anglica* (Oenema & DeLaune 1988). Unvegetated sites i.e., pan sediments in the low marsh were highly reducing (Eh – 100 mV or lower) at depths greater

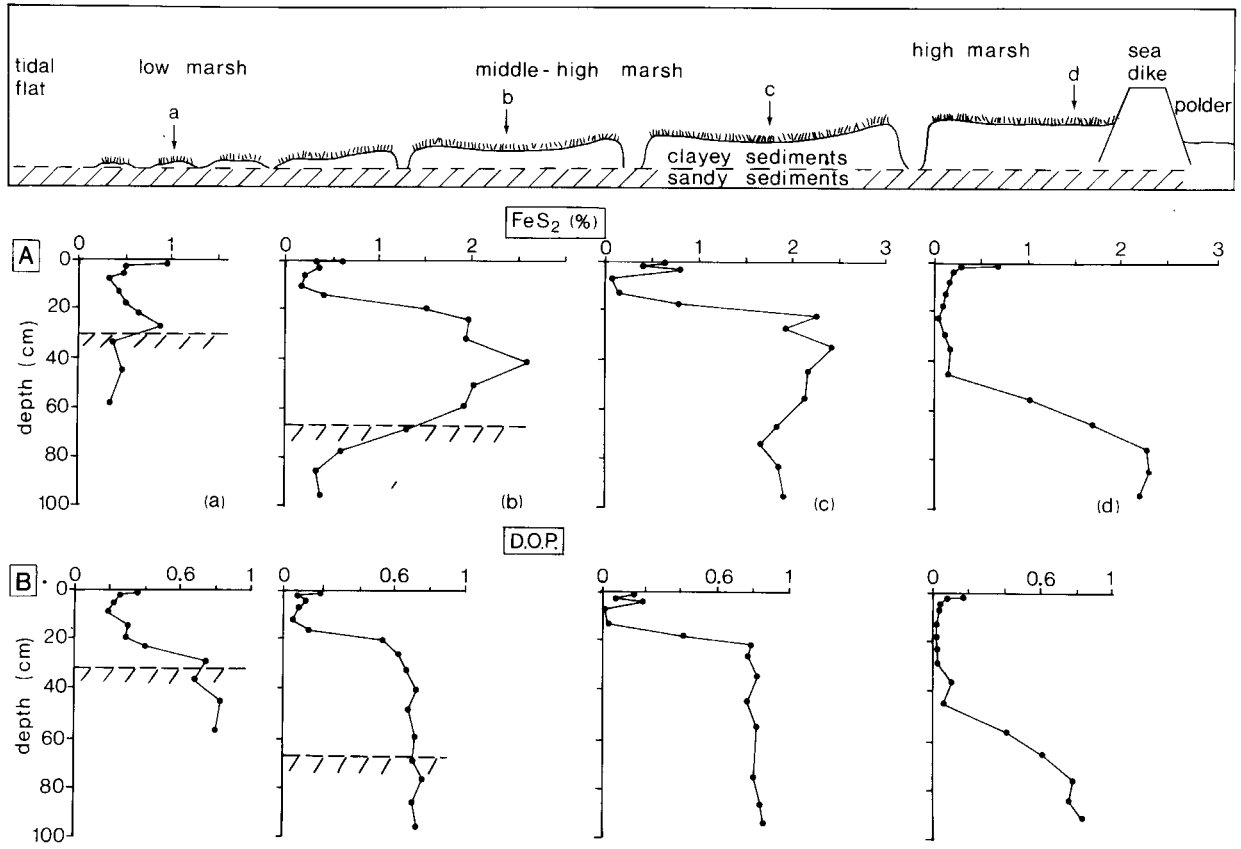

Fig. 3. Cross-section of the Rattekaai marsh. Arrows (a–d) indicate sampling sites. (*A*) depth distribution of FeS_2 and (*B*) depth distribution of the degree of pyritization (DOP). Broken lines indicate depth of sandy tidal flat sediments. Cores from October 1984.

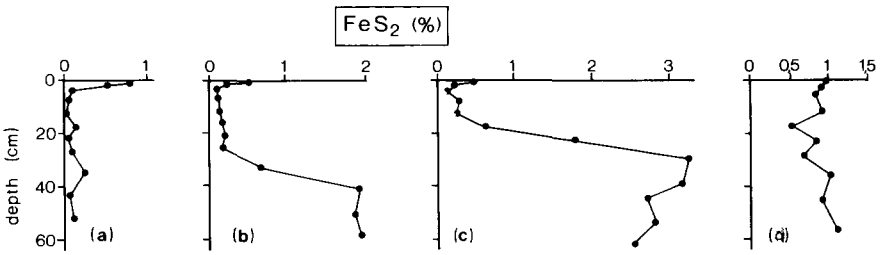

Fig. 4. Depth distribution of FeS_2 in sediments of the medium-high Rattekaai marsh at varying distances from a creek. (*a*) 1 m. (*b*) 9 m. (*c*) 15 m. and (*d*) in a pan-sediment from an abandoned creek. (May 1985).

than 1 cm. Such differences between bare and vegetated sites were also found by Howes et al. (1981) and are consistent with the observed FeS_2 profiles (Figs. 3, 4) and pore water chemistry (see below).

Pyrite was formed at the interface of the oxidized and underlying reduced sediment. The formation was restricted to a rather narrow depth interval; in the low and medium high marsh at 15–20 cm and in the high marsh at 40–50 cm. Below this FeS_2 formation zone, no further increases in FeS_2 concentration occurred, and there were even some decreases, which were related to the lower concentrations of clay, silt and organic carbon at greater depths. Figure 3 shows the low FeS_2 concentrations in the low marsh and the sharp decrease in FeS_2 concentration between 50–70 cm in the medium-high marsh, coinciding with the depth of the sandy sediments of the underlying tidal flat. The calculated net rate of pyrite formation below a depth of 15 cm in the sediments of the medium-high marsh equalled 2.6–3.8 mol S-FeS_2 m^{-2} yr^{-1}, using a FeS_2 concentration of 2–3% (Figs. 3, 4), a sedimentation rate

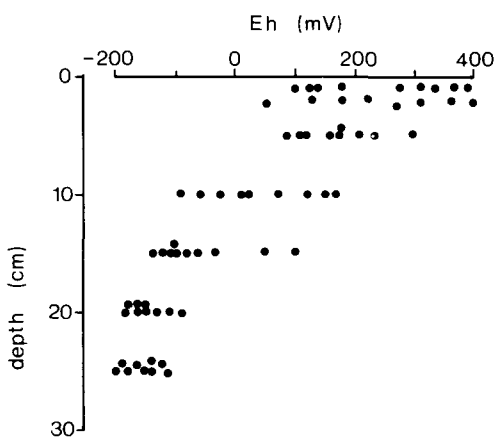

Fig. 5. Results of Eh measurements in the medium-high marsh (Febr. 1985–May 1986).

Table 1. Characteristics of backmarshes in the low, medium-high and high Rattekaai salt marsh.

	Low	Medium-high	High
Flooding frequency before 1984 (yr^{-1})	620–550	550–120	< 120
Flooding frequency in 1985 (yr^{-1})	520–410	410–100	< 100
Flooding frequency in 1986 (yr^{-1})	270–100	100–16	< 16
Mean water table depth in 1984 (cm)	0–10	10–15	> 30
Mean water table depth in 1985 (cm)	0–15	10–20	> 40
Mean water table depth in 1986 (cm)	10–40	10–40	> 40
Clay content (%)	5–20	30–50	30–50
Organic carbon content (%)	1–4	5–7	5–7
Porosity (%)	50–70	70–85	60–80

of 1.5 cm yr^{-1} (Oenema & DeLaune 1988) and a bulk density of 0.5 g cm^{-3}. Since on average 2 mol organic carbon are oxidized for every mol of SO_4 reduced, 60–90 g C m^{-2} yr^{-1} needed to be respired annually by the sulfate reducers to account for the observed FeS_2 accumulation. This is only a small portion (< 4%) of the estimated annual below-ground carbon input by root biomass production (Groenendijk 1987).

Unvegetated marsh sediments, such as the reducing deposits in abandoned creeks (Fig. 4d), contained only 0.5–1% FeS_2, and the slight variations with depth were related to variations in the clay + silt and organic carbon content. The straight pyrite profiles and the relatively low pyrite concentrations strongly suggest that both the oxidation of detrital pyrite in the surface layer and the in-situ FeS_2 formation below this layer were negligible.

Seasonal variations in the FeS_2 profiles were small. Similar small seasonal variations were observed in sediments of Great Marsh, Delaware by Lord (1980). Large seasonal variations in FeS_2 concentrations at 0–30 cm in sediments of Sippewissett Marsh, Massachusetts were reported to be related to seasonal variations in the metabolism of the roots of *Spartina alterniflora* (Howarth & Teal 1979). Feijtel et al. (1988) demonstrated the dominant influence of tide dynamics on redox conditions and pyrite accumulation in Louisiana salt marshes. The great differences between seasonal cycles of pyrite accumulation in different regions clearly illustrate the complexity of marsh geochemistry, particularly in the formation of pyrite in sediments.

Pyrite mineralogy

Abundant pyrite particles were found in the reducing sediment by incident light and scanning electron microscopy. The pyrite particles were found as

Plate 1. S.E.M. micrographs of framboidal pyrite. ⟶

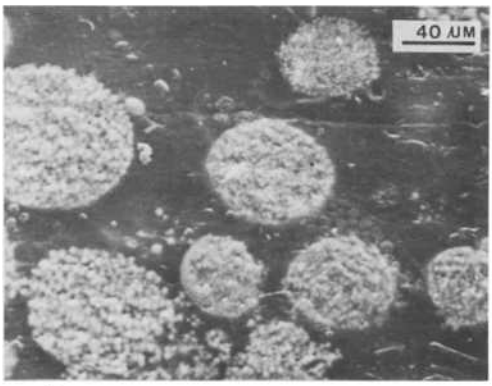

A

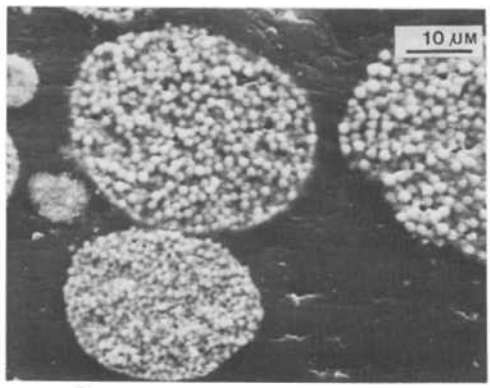

B

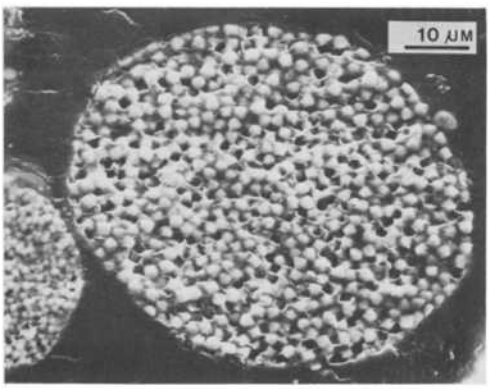

C

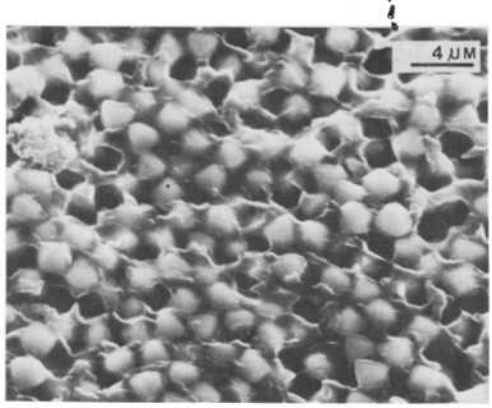

D

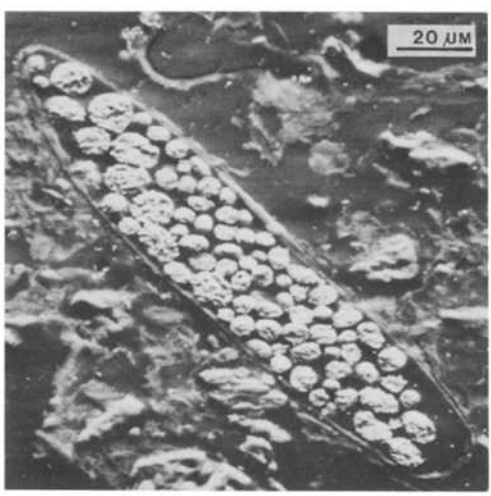

E

framboids ranging from 5–70 micrometers in diameter (Plate 1). Most of the framboids were clustered in and around roots and diatoms, as observed by Miedema et al. (1974), Kooistra (1981), and Luther et al. (1982). The single crystals within framboids were equal in size, but varied greatly (0.5–5 μm) between different framboids. The crystals had an irregularly spherical shape (Plate 1D). A few disseminated single crystals were observed, but these were probably artifacts of sample polishing. Note the disruption of the surface of several framboids.

Framboidal pyrite is widespread in marine sediments. It is found in sediments where the pyrite is formed via intermediates of iron monosulfides and greigite (Berner 1970; Sweeney & Kaplan 1973). Euhedral single crystals are believed to form when pyrite is synthesized directly (Rickard 1975; Howarth 1979; Luther et al. 1982). Such small (0.1–2 μm) euhedral pyrite particles may form very rapidly in salt marshes (Howarth 1979). The abundance of framboids in the marshes of the Eastern Scheldt suggests the indirect formation of pyrite through iron monosulfide precursors.

Red and dark brown patches of iron oxyhydroxide, many of them surrounding roots and pores, were observed in the oxidized surface sediments. Several dark brown nodules had a framboid-like shape with a pyrite nucleus remaining inside. Most of these oxidized framboids were observed in the surface (0–1 cm) layer and at the interface of the oxidizing and reducing sediments, at a depth of 13–15 cm in the medium high marsh. This latter observation reflected the lowering of the mean depth of the water table in 1986 (Table 1).

The slow oxidation of the detrital pyrite as observed in the suspended matter and in the superficial sediment of the salt marshes is probably related to the relatively small surface area of the large framboids (e.g., Pugh et al. 1984). Large seasonal variations in pyrite concentrations were observed in salt marshes with small euhedral crystals (Howarth & Teal 1979; Luther et al. 1982; Feijtel et al. 1988). These crystals were 10–100 times smaller than the framboids observed in the sediments of the Rattekaai marsh. Framboidal pyrite was associated with only small seasonal variations in FeS_2 concentrations in the Great Marsh, Delaware (Lord 1980) as well as in the present study sites.

Hydrological observations

The mean depth of the water table in the backmarshes of Rattekaai was related to the flooding frequency (Table 1) and surface topography. Unvegetated sites in pan-sediments form depressions in the low and medium-high marsh and were flooded for almost the whole year (before 1985), but

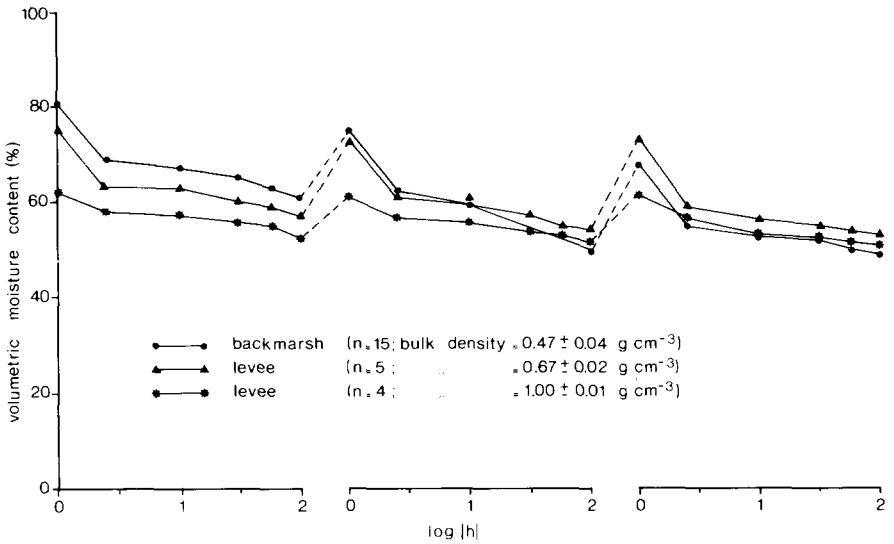

Fig. 6. Moisture retention curves of backmarsh- and levee samples from the medium-high marsh. Results of three successive cycles in the range $\log|h| = 0$ to $\log|h| = 2$.

the vegetated sites rapidly drained by surface run-off at low tide. After flooding, the water table typically fell within one day to about 10 cm below the surface in the backmarsh sediments. Rapid downward movement of the water table in salt marsh sediments has been ascribed to water-uptake and evapotranspiration (Hemond & Fifield 1982; Dacey & Howes 1984; Hemond et al. 1984) and to drainage during low tide (e.g., Howarth et al. 1983). Results presented in Fig. 6 indicate a great loss of pore water (10–13%), from saturation to a matrix suction of only 2.5 cm ($\log|h| = 0.4$). This great loss was mainly caused by drainage through root channels. A total of 12–15% soil water drained at a matrix suction of 10 cm. A further increase in matrix suction from 10 to 100 cm caused another 5% of pore water to be drained. Through this latter drainage the unconsolidated backmarsh sediments lost their capacity to reabsorb all the initially drained water during a subsequent inundation (Fig. 6). However, when the matrix suction did not exceed about 10 cm the sediments kept a high water holding capacity (not shown). Thus, backmarsh sediments remained unconsolidated in the surface layers as long as the downward movement of the water table did not exceed about 10 cm. The increased downward movement of the water table in 1986 (Table 1) irreversibly decreased the water holding capacity of the backmarsh sediments and led to a subsidence of 1–5 cm in the backmarshes.

Evidence for drainage at low tide was obtained from measurements of pore water seepage through creek banks. However, the mean seepage rate,

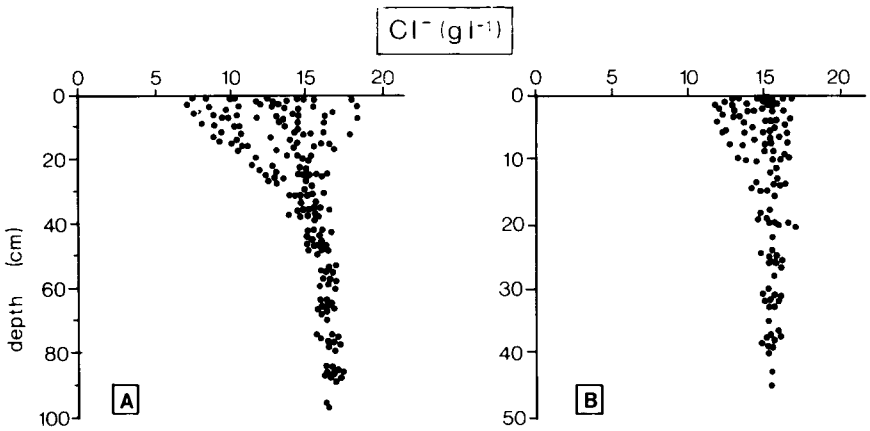

Fig. 7. Variation in Cl^- concentrations in pore waters of (*A*) the medium-high and (*B*) the low marsh (October '84–May '86).

estimated from the results of the seepage measurements (0–170 ml m^{-1} hr^{-1}), and the mean length of the creeks per m^2 marsh were far too small (< 20%) to account for the rapid water loss in the top 10 cm after flooding. An additional but unknown portion may be lost via surface run-off or downward flow into the underlying sandy sediments and interflow to the creek bottoms (e.g., Hemond et al. 1984; Jordan & Correl 1985). The chloride concentration of the seepage water (9–14 g l^{-1}, n = 31) fell in the same range as that of the pore waters in the top 10 cm (11–13 g l^{-1}) of the backmarsh sediments. The seasonally averaged Cl^- concentration at 30–100 cm was significantly higher (see below). This suggests lateral drainage of pore water from surface layers only.

Pore water composition

The variations in pore water Cl^- concentration of the low and medium-high marsh are shown in Fig. 7. The Cl^- concentration in the surface layers responds to changes taking place at and near the surface of the marsh. Such changes are caused by inundation, evapotranspiration and infiltration of rain water. The chloride oscillations in the surface layers of the low marsh (14–16 g l^{-1}) and the medium-high marsh (12–17 g l^{-1}) were much smaller in 1984–1985 than in 1986. The increased influence of rainfall and evapotranspiration in 1986 decreased the Cl^- concentration in the surface layers of the medium-high marsh to as low as 7 g l^{-1} in May.

With increasing depth in the sediment the variations in Cl^- concentration damped out and approached the seasonally averaged Cl^- concentration (Lord & Church 1983; Casey & Lasaga 1987). The similarity between the

seasonally averaged Cl^- concentration in the medium-high marsh ($16.5\,g\,l^{-1}$), the low marsh ($15.5\,g\,l^{-1}$) and the inundation water ($15–16\,g\,l^{-1}$), suggests that the Cl^- concentration in the subsurface of backmarsh sediments are predominantly controlled by seawater inundation. The differences in atmospheric exposure between the medium-high and low marsh (Table 1) and the excess of precipitation over evapotranspiration of $20\,cm\,yr^{-1}$ in the Netherlands had only a minor influence. In contrast, Casey & Lasaga (1987) and Lord & Church (1983) reported that the seasonally averaged salinity in marsh sediments in Virginia and Delaware were 2.3 and 1.7 times higher than in the mean floodwater.

Seasonal variations in SO_4^{2-} concentrations in the medium-high marsh are shown in Fig. 8. SO_4^{2-} data were normalized to a time-averaged Cl^- concentration of $16\,g\,l^{-1}$ to negate atmospheric effects (precipitation, evapotranspiration) according to:

$$SO_4^{2-}(n) = SO_4^{2-}(x) * Cl^-(\text{av})/Cl^-(x) \quad (2)$$

where $SO_4^{2-}(n)$ = normalized SO_4^{2-} concentration at depth x,

$SO_4^{2-}(x)$ = measured SO_4^{2-} concentration at depth x,

$Cl^-(\text{av})$ = time-averaged Cl^- concentration at depth x,

$Cl^-(x)$ = measured Cl^- concentration at depth x.

The time-averaged seawater SO_4^{2-} concentration is indicated by the dotted line in Fig. 8. In 1985, SO_4^{2-} profiles were relatively unaffected by the reduction in flooding frequency and were comparable to profiles measured in 1984. In the top 5–20 cm a slight sulfate-enrichment occurred because of the oxidation of pyrite and upwardly diffusing dissolved sulfides. The significant increase in 1986 of the sulfate-enrichment at 15–30 cm was caused by pyrite oxidation. Pyrite oxidation was most intense in the late summer, when SO_4^{2-} and Fe concentrations as high as 70 mM and 2.7 mM, respectively, and pH values as low as 2.7–3.5 were observed (Figs. 8, 9). The sulfate-depletion below a depth of 10–30 cm indicates net sulfate reduction.

The dissolved Fe^{2+} and ΣS profiles of the medium-high marsh (Fig. 9) generally are similar to those reported for permanently submerged marine sediments (e.g., Aller 1980; Sørensen & Jørgensen 1987). The subsurface peak of dissolved Fe^{2+} was pronounced, with maximum concentrations of $750\,\mu M$ during summer and fall. Equally high Fe^{2+} concentrations have been reported for the Great Marsh by Lord (1980), but Fe^{2+} concentrations in the pore waters of the surface layers in the Sippewisset Marsh were more than 10 times lower (Giblin & Howarth 1984). Above the subsurface peak the Fe^{2+} concentrations were controlled by oxidation of upwardly diffusing

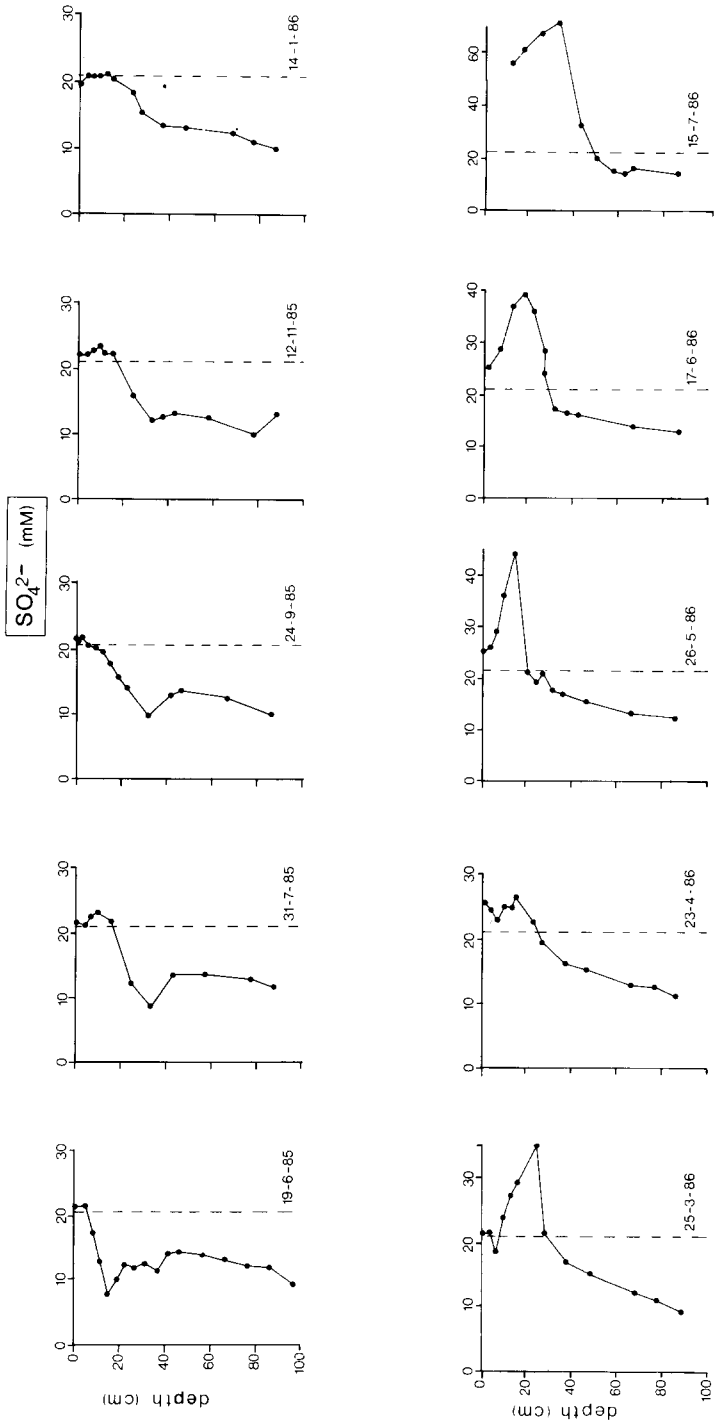

Fig. 8. Seasonal variation in dissolved SO_4^{2-} in the pore waters of the medium-high marsh. Dotted line indicates inherent seawater sulfate concentration at a mean Cl^- concentration of 16 g l^{-1}.

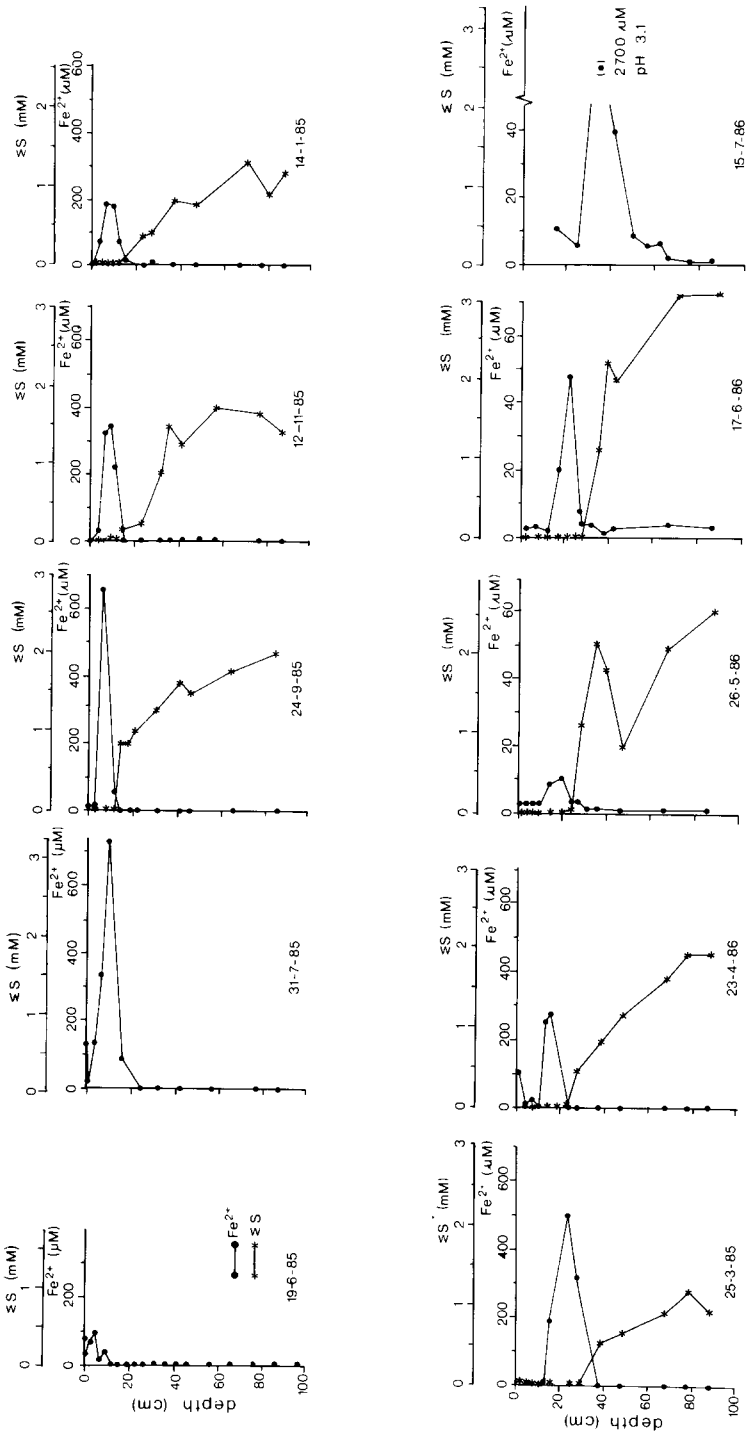

Fig. 9. Seasonal variations in dissolved Fe and ΣS in the pore waters of the medium-high marsh.

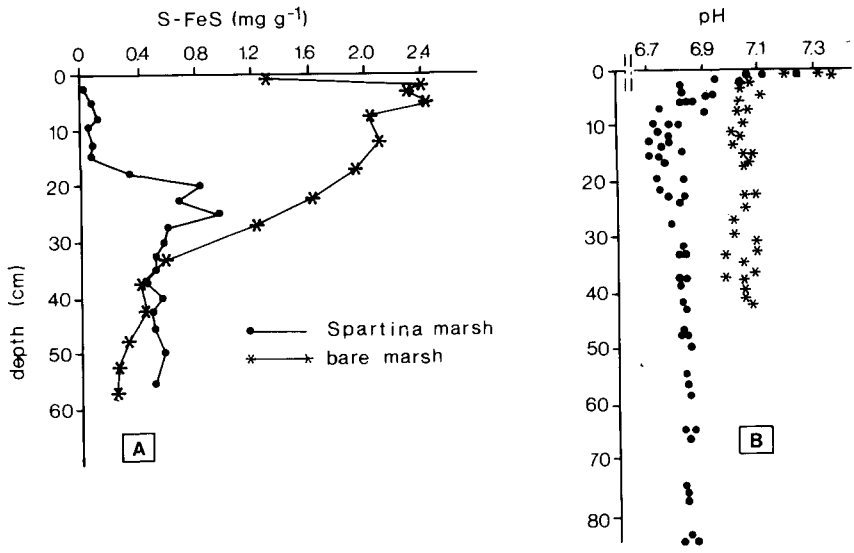

Fig. 10. Depth distribution of (*A*) AVS (acid volatile sulfides) and (*B*) pH in a Spartina anglica-supporting medium-high marsh and in a pan-sediment of the low-marsh.

ferrous iron to ferric iron. The low solubility of iron sulfides controlled the invariably low ($< 5\,\mu M$) Fe^{2+} concentration in the sulfidic sediment.

Acid volatile sulfides (AVS) were found throughout the sediment (Fig. 10), but in significant concentrations ($600\,\mu g\,g^{-1}$ S-FeS) only in the dissolved sulfide-containing sediment. The presence of AVS in the oxidized surface layer suggests the accumulation of sulfides in microniches (Jørgensen 1977). Data of Lord (1980) show high AVS (0.2–0.4% S-FeS) and low pyrite concentrations in the surface layers (0–8 cm) of Great Marsh, Delaware, and low AVS ($\ll 0.1\%$) concentrations in the underlying pyritic sediment. Very low AVS ($< 16\,\mu g$ S-FeS g^{-1} dry wt.) and very high pyrite concentrations (6–9%) were reported by Howarth & Teal (1979) for surface sediments (0–30 cm) of Sippewissett Marsh in Massachusetts. There is as yet no satisfactory explanation for these great differences in AVS and pyrite profiles, but differences in pH and redox conditions are probably involved.

Pore water SO_4^{2-}, Fe^{2+} and ΣS profiles for the bare sediment were different from those for sediments in the marsh overgrown with *Spartina anglica*. In the pan sediment the SO_4^{2-} concentration decreased rapidly with depth (Fig. 11A). The increase below 20 cm was caused by upwardly diffusing SO_4^{2-} from the underlying sandy sediments (Oenema 1988a). Concentrations of Fe^{2+} were invariably low ($< 5\,\mu M$) at depths of > 1 cm in the pan sediments, because of the precipitation of iron monosulfides (Fig. 10A). The

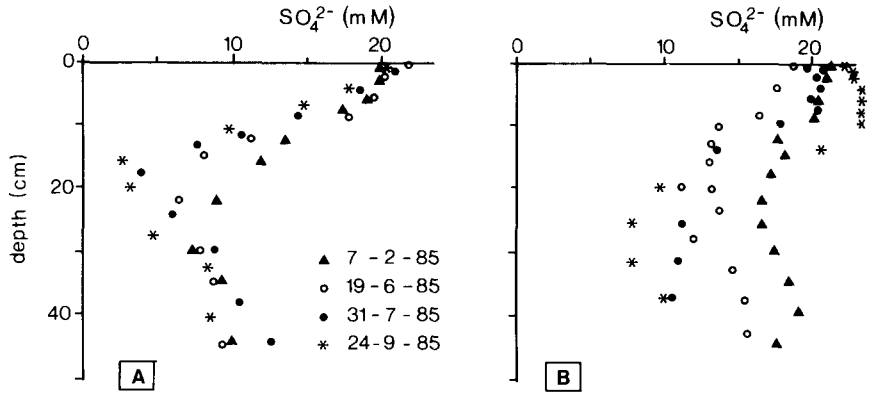

Fig. 11. Seasonal variation in dissolved SO_4^{2-} in the pore waters of sediments from the low marsh. (*A*) a pan-sediment and (*B*) a Spartina anglica-supporting sediment.

overgrown site in the low marsh showed great seasonal variations in SO_4^{2-} concentration at 0–15 cm (Fig. 11B). In early summer SO_4^{2-} was depleted, but as *Spartina anglica* reached maturity the pore waters were enriched with SO_4^{2-}. Dissolved ΣS concentrations were variable, but low ($< 40\,\mu M$) at 0–15 cm. Below this dynamic surface layer, ΣS increased to maxima of $200\,\mu M$ at 30–40 cm which is still 10–20 times smaller than in the pan-sediments. These observations clearly illustrate the differences between the geochemistry of overgrown and bare marsh sediments. Even though the supply of decomposable organic carbon in overgrown sites is much larger than in pan-sediments, the sulfate-depletion and the concentrations of dissolved ΣS were much larger in the latter sediments.

Control of FeS_2 formation

The abundance of pyrite framboids and the relatively high AVS and dissolved ΣS concentrations in the reducing marsh sediments all point to the formation of pyrite through amorphous iron monosulfides, mackinawite and greigite intermediates (Berner 1970; Sweeney & Kaplan 1973; Rickard 1975). Appropriate conditions for pyrite formation apparently occur in a narrow range of depths, where the dissolved Fe^{2+} and ΣS profiles intersect (cf. Figs. 3 and 9). A part of the ΣS reacts with Fe^{2+} to form iron monosulfides (Fig. 10A), another part may oxidize to elemental sulfur (S^0), polysulfides and sulfate. Further reaction of FeS with S^0 finally produces pyrite.

There are three possible reasons why the conversion of FeS into FeS_2 was rapidly at the interface of the oxidizing and reducing sediment of *Spartina* overgrown stands but not in bare sediments.

1. Roots create local oxidizing conditions (e.g., Gleason & Zieman 1981; Mendelsohn et al. 1981), that promote oxidation of sulfides to elemental sulfur.
2. The drainage characteristics (Fig. 6) combined with the seasonal growth dynamics of *Spartina anglica* promote an up and down shifting of the (sub)oxic-anoxic boundary in overgrown-marsh sediments. This shifting causes a temporal oxidation of reduced sulfur species at the interface, and so may promote the formation of S^0 and FeS_2.
3. A slightly lower pH (0.2–0.3 units) in overgrown sediments (Fig. 10B) also promotes pyrite formation (Rickard 1975).

The close association of pyrite framboids with plant roots (see also Miedema et al. 1974; Luther et al. 1982; Feijtel et al. 1988) focusses attention on the rhizosphere. This environment may provide room for the growing framboid clusters, stimulate growth of sulfate-reducing bacteria by releasing metabolizable substrates, and stimulate pyrite formation directly by the locally oxidizing and acidic conditions. Possible acidic conditions in the rhizosphere were inferred from the alkaline nutrient by *Spartina anglica* (Oenema 1988a). The observation that the concentration of dissolved ΣS and AVS, but also of NH_4^+ and ΣPO_4 sharply increased below the zone of FeS_2 formation (results unpubl.), eventhough the roots extended to depths of 60 cm or more (Groenendijk 1987; Oenema & DeLaune 1988) is consisted with the proposed role of active roots in pyrite formation.

The availability of dissolved sulfate, metabolizable organic carbon and reducible iron ultimately control how much pyrite can form (Goldhaber & Kaplan 1974; Berner 1984). In the sediments of the Rattekaai marsh dissolved SO_4^{2-} is not the limiting factor for sulfate reduction or pyrite formation, since the concentrations always exceeded 5 mM. The control of pyrite formation by organic carbon is generally suggested by their linear relationship (Berner 1982; Raiswell & Berner 1985). This relationship implies that a constant proportion of the organic carbon deposited was oxidized by bacterial sulfate reduction, and that also a constant proportion of the produced sulfide was converted to pyrite. Both the contribution of sulfate reducers to organic carbon oxidation and the percentage of bacterially reduced sulfide trapped in marine sediments are related to the sedimentation rate and have been found to range from 1–70% (Berner 1978; Jørgensen 1982; Chanton et al. 1987). Despite this variance there is a fairly constant C/S ratio (organic carbon to S-FeS_2 on a weight basis) of 2.8 ± 0.8 in a number of marine sediments. (Goldhaber & Kaplan 1975; Berner 1982). In the reducing part of marsh sediments in the Eastern Scheldt, the organic carbon concentration varied between 0.8 and 7.1% and the C/S ratio

between 3.5 and 6.3, with a mean of 4.2. The high C/S ratio may reflect in part the presence of land-derived refractory organic carbon (Oenema 1989), but since the concentrations of organic C and detrital Fe were related, there may be also shortage of easily reducible iron.

Lord and Church (1983) ascribed the slow pyrite formation and the very low AVS concentration below a depth of 9 cm in sediments of the Great Marsh to the slow dissolution of refractory ferric iron. In the sediments of the Eastern Scheldt marshes, the oxalate-extractable Fe (Fe_{ox}) concentrations decreased from 1–2% in the oxidized surface layers to 0.1–0.5 in the sulfidic sediment (Fig. 2). Only a minor part of this depth variation was related to a subsurface enrichment of iron: Fe/Al (XRF) ratios at 0–5 cm were slightly higher than those below 15 cm. The major part of the depth variation in Fe_{ox} was due to pyrite formation. DOP values increase from < 0.3 in the oxidized surface layers to approximately 0.7–0.8 in the reducing layers (Fig. 3B). The constancy of the DOP in the reducing sediments, indicates that only 70–80% of Fe_{ox} was readily available for pyrite formation. A part of the residual 20–30% Fe_{ox} was tied up with the AVS (0.1–0.2% Fe; Fig. 9A). Another part was apparently not readily accessible for sulfidation because of its larger crystal grains (Rickard 1974; Pyzik & Sommer 1981).

The data so far do not allow to conclude whether shortage of reducible Fe or the absence of an active root system limits further pyrite formation below a depth of about 20 cm in the medium-high marsh.

Acknowledgements

I would like to thank Mark van Alphen, Vian Govers and Hein Craanen for assistance with the analyses of AVS, pyrite and major elements (XRF). The pore waters were analyzed at the laboratory of Rijkswaterstaat, Tidal Waters Division, Middelburg.

The comments of drs T.C. Feijtel, F.R. Moormann and C.H. van der Weijden and two anonymous reviewers are greatly appreciated. This research was carried out at the Institute of Earth Sciences, University of Utrecht and supported by the Delta Department of the Ministry of Transport and Public Works.

References

Aller RC (1980) Diagenetic processes near the sediment-water interface of Long Island Sound. II Fe and Mn. Adv. Geophys. 22: 351–415

Bassett J, Denney RC, Jeffery GH & Mendham J (1978) Vogel's Textbook of Quantitative Inorganic Analysis. Longman Inc. New York, 925 pp.

Begheyn L Th, Van Breemen N & Veldhorst EJ (1978) Analysis of sulfur compounds in acid sulfate soils and other recent marine soils. Comm. Soil Sc. Plant Anal. 9: 873–882

Berner RA (1970) Sedimentary pyrite formation. Am. J. Sci. 268: 1–23

——— (1978) Sulfate reduction and the rate of deposition of marine sediments. Earth Planet. Sc. Lett. 37: 492–498

——— (1982) Burial of organic carbon and pyrite sulfur in the modern ocean: its geochemical and environmental significance. Am. J. Sci. 282: 451–473

——— (1984) Sedimentary pyrite formation; an update. Geochim. Cosmochim. Acta. 48: 605–615

Breemen N van (1976) Genesis and solution chemistry of acid sulfate soils in Thailand. PhD diss., Agric. Univ., Wageningen, 263 pp.

Breemen N van, Driscole CJ & Mulder J (1983) Acidification and alkalinization of soils. Plant and Soil 75: 283–308

Casey WH & Lasaga AC (1987) Modeling solute transport and sulfate reduction in marsh sediments. Geochim. Cosmochim. Acta 51: 1109–1120

Chanton JP, Martens CS & Goldhaber MB (1987) Biogeochemical cycling in an organic rich coastal marine basin. 7. Sulfur mass balance, oxygen uptake and sulfide retention. Geochim. Cosmochim. Acta. 51: 1187–1199

Dacey JWH & Howes BL (1984) Water uptake by roots controls water table movement and sediment oxidation in short *Spartina* marsh. Science 224: 487–489

Feytel TC, DeLaune RD & Pattrick WH (1988) Seasonal pore water dynamics of Barataria Basin, Louisiana. Soil. Sci. Soc. Am. J. 52: 59–67

Giblin AE & Howarth RW (1984) Pore water evidence for a dynamic sedimentary iron cycle in salt marshes. Limnol. Oceanogr. 29: 47–63

Gilboa-Garber N (1971) Direct spectrophotometric determination of inorganic sulfide in biological materials and in other complex mixtures. Anal. Biochem. 43: 129–133

Gleason ML & Zieman JC (1981) Influence of tidal inundation on internal oxygen supply of Spartina alterniflora and Spartina patens. Est. Coast. Shelf. Sci. 13: 47–57

Goldhaber MB & Kaplan IR (1974) The sulfur cycle. In: Goldberg ED (Ed) The Sea, vol 5 (pp 569–655) John Wiley & Sons. New York

Goldhaber MB & Kaplan IR (1975) Controls and consequences of sulfate reduction in recent marine sediments. Soil Sci. 119: 42–55

Groenendijk A (1987) Ecological consequences of a storm-surge barrier in the Oosterschelde: the salt marshes, PhD diss., Univ. of Utrecht, 177 pp.

Hemond HF & Fifield JL (1982) Subtidal flow in salt marsh peat: A field and model study. Limnol. Oceanogr. 27: 126–136

Hemond HF, Nuttle WK, Burke RW & Stolzenback KD (1984) Surface infiltration in salt marshes: Theory, measurements and biogeochemical implications. Water Resources Res. 20: 591–600

Henriksen A (1967) An automated method for the determination of iron. Vattenhygièn. May 22 (1967): 1–8

Hesslein RH (1976) An in-situ sampler for close interval pore studies. Limnol. Oceanogr. 21: 912–914

Holmgren GGS (1967) A rapid citrate-dithionite extractable iron procedure. Proc. Soil Sci. Soc. Am. 31: 210–211

Howarth RW (1979) Pyrite: its rapid formation in a salt marsh and its importance in ecosystem metabolism. Science 203: 49–51

Howarth RW (1984) The ecological significance of sulfur in the energy dynamics of saltmarsh and coastal marine sediments. Biogeochem. 1: 5–27

Howarth RW & Teal JM (1979) Sulfate reduction in a New England salt marsh. Limnol. Oceanogr. 24: 999–1014

Howarth RW, Giblin A, Gale J, Peterson BJ & Luther GW (1983) Reduced sulfur components in the pore waters of a New England salt marsh. Ecol. Bull. 35: 135–152

Howes BL, Howarth RW, Teal JM & Valiela I (1981) Oxidation-reduction potentials in a salt marsh: Spatial patterns and interactions with primary production. Limnol. Oceanogr. 26: 350–360

Howes BL, Dacey JWH & King GM (1984) Carbon flow through oxygen and sulfate reduction pathways in salt marsh sediments. Limnol. Oceanogr. 29: 1037–1051

Jordan TE & Correl DL (1985) Nutrient chemistry and hydrology of interstitial water in brackish tidal marshes of Chesapeake Bay. Est. Coast. Shelf. Sci. 21: 45–55

Jørgensen BB (1977) Bacterial sulfate reduction within reduced microniches of oxidized marine sediments. Mar. Biol. 41: 7–17

Jørgensen BB (1982) Mineralisation of organic matter in the sea-bed; the role of SO_4^{2-} reduction. Nature. 296: 643–645

Klute A, Ed (1986) Methods of Soil Analysis. Part 1. Physical and Mineralogical Methods. 2nd ed. Agronomy 9. SSSA, Wisconsin. 1188 pp.

Knoester M, Visser J, Bannink BA, Colijn CJ & Broeders WPA (1984) The Eastern Scheldt project. Wat. Sci. Techn. 16: 51–77

Kooistra MJ (1978) Soil development in recent marine sediments of the intertidal zone in the Oosterschelde. Soil Survey Papers. 14. Soil Survey Institute, Wageningen. 183 pp.

Kooistra MJ (1981) The determination of Fe, Mn, S and P in thin sections of recent marine intertidal sediments in S.W. Netherlands by SEM-EDXRA. In: Bisdom EBA (Ed) Submicroscopy of Soils and Weathered Rocks (pp. 217–236) Pudoc, Wageningen

Lord CJ (1980) The chemistry and cycling of iron, manganese and sulfur in salt marsh sediment. PhD diss., Univ. Delaware, Newark., 177 pp.

Lord CJ & Church TM (1983) The geochemistry of salt marshes: sedimentary ion diffusion, sulfate reduction and pyritization. Geochim. Cosmochim. Acta 47: 1381–1391

Luther GW, Giblin A, Howarth RW & Ryans RA (1982) Pyrite and oxidized iron mineral phases formed from pyrite oxidation in salt marsh and estuarine sediments. Geochim. Cosmochim. Acta 46: 2665–2669

Mendelssohn IA, McKee KL & Patrick WH (1981) Oxygen deficiency in Spartina alterniflora roots: Metabolic adaptions to anoxia. Science 214: 439–441

Merks AGA & Sinke JJ (1981) Application of an automated method for dissolved sulfate analysis to marine and brackish waters. Mar. Chem. 10: 103–108

Miedema R, Jonghams AG & Slager S (1974) Micromorphological observations on pyrite and its oxidation products in four Holocene aluvial soils in the Netherlands. In: Rutherford GK (Ed) Soil Microscopy, Proc. of the 4th Int. Working Meeting on Soil Microscopy (pp 772–794) Limestone Press, Kingston

Oenema O (1988a) Early diagenesis in recent fine-grained sediments in the Eastern Scheldt. PhD diss., Univ. of Utrecht, 223 pp.

——— (1988b) Diagenesis in subrecent marine sediments in the Eastern Scheldt, Southwest Netherlands. Neth. J. Sea Res. 22: 253–265

——— (1989) Distribution and cycling of recent fine-grained sediments in the eastern Scheldt, Southwest Netherlands. Geol. Mijnbouw. 68: 189–200

Oenema O & DeLaune RD (1988) Accretion rates in salt marshes of the Eastern Scheldt, Southwest Netherlands. Est. Coast. Mar. Sci. 26: 379–394

Page AL, Millar RH & Keeney DR, Eds (1982) Methods of Soil Analysis. Part 2. Chemical and Mineralogical Properties. 2nd ed. Agronomy 9 (2). S.S.S.A. Madison, Wisconsin, 1159 pp.

Phillips EJP & Lovley DR (1987) Determination of Fe(III) and Fe(II) in oxalate extracts of sediments. Soil Sci. Soc. Am. J. 51: 938–941

Pugh CE, Hossner LR & Dixon JB (1984) Oxidation rate of iron sulfides as affected by surface area, morphology, oxygen concentration and autotrophic bacteria. Soil Sci. 137: 309–314

Raiswell R (1982) Pyrite texture, isotopic composition and the availability of iron. Am. J. Sci. 282: 1244–1263

Raiswell R & Berner RA (1985) Pyrite formation in euxinic and semi-euxinic sediments. Am. J. Sci. 285: 710–724

Rickard DT (1974) Kinetics and mechanism of the sulfidation of goethite. Am. J. Sci. 274: 941–952

Rickard DT (1975) Kinetics and mechanism of pyrite formation at low temperature. Am. J. Sci. 275: 636–652

Schulze DG (1981) Identification of soil iron oxide minerals by XRD. Soil. Sci. Soc. Am. J. 45: 437–440

Schwertmann U (1964) Differenzierung der Eisenoxide des Bodens durch Extraction mit Ammoniumoxalat-Lösung. Z. Pflanzenernähr. Dung. Bodenkunde. 105: 194–203

Sørensen J & Jørgensen BB (1987) Early diagenesis in sediments from Danish coastal waters: microbial activity and Mn-Fe-S geochemistry. Geochim. Cosmochim. Acta. 51: 1583–1590

Sweeney RE & Kaplan IR (1973) Pyrite framboid formation: Laboratory synthesis and marine sediments. Econ. Geol. 68: 618–634